ISTITUTO NAZIONALE DI FISICA NUCLEARE

Sezione di Trieste

INFN/AE-92/12

24 marzo 1992

G. Ballocchi, A. Castoldi, S. Chinnici, P.T. Cox, E. Gatti, P. Giacomelli, P. Holl, J. Kemmer, A. Longoni, F. Palma, P. Rehak, M. Sampietro and A. Vacchi

BEAM TEST OF A LARGE AREA SILICON DRIFT DETECTOR

Servizio Documentazione
dei Laboratori Nazionali di Frascati

BEAM TEST OF A LARGE AREA SILICON DRIFT DETECTOR

A. Castoldi, S. Chinnici[1], E. Gatti, A. Longoni, F. Palma[2], M. Sampietro
Politecnico di Milano, Dipartimento di Elettronica Quantistica e Strumentazione Elettronica
CNR, Milano Italy

P. Rehak
Brookhaven National laboratory, Upton, NY, USA

G. Ballocchi[3]
CERN, PPE division, 1211, Geneve CH

J. Kemmer
TU Munchen 8046 Garching and
Ketek GmbH, Hauptstrasse 41d, 8048 Haimhausen Germany

P. Holl
Ketek GmbH, Hauptstrasse 41d, 8048 Haimhausen Germany

P.T. Cox, P. Giacomelli[4], A. Vacchi[5]
The Rockefeller University New York NY 10021 USA

Abstract

The results from the tests of the first large area (4 x 4 cm^2) planar silicon drift detector prototype in a pion beam are reported. The measured position resolution in the drift direction is $\sigma=(40 \pm 10)\mu m$.

---

[1]Now at Telettra S.p.A., Vimercate, Italy.
[2]Now at Laben, Milano Italy.
[3]Now at The University of Michigan, Ann Arbor, Michigan USA.
[4]Now at CERN, Geneve Switzerland .
[5]Now at INFN Trieste, Trieste Italy.

determined the position of the particle to±50μm. The SiDD was mounted on a remotely controlled x y stage movable by stepping motors.

The detector and the read-out electronics

All measurements were performed with the multi-anode linear drift detector whose schematic layout is shown in fig.1 , [ref 4, 5]. This is a square detector made of 300 μm thick, 2 kΩcm FZ n-type silicon. The sensitive area of the detector (about 4 x 4 cm^2) is divided into two parts, with electrons drifting in opposite directions from the centre toward two rows of 166 anode each. This allows to reduce the maximum drift length and the biasing voltages. The detector is provided with an implanted voltage divider and is implemented with injecting electrodes allowing drift velocity calibration [6]. During the tests the whole detector was polarized, but only part of it was implemented with read-out electronics. The read-out anodes, spaced 200 μm apart, were connected two by two, so that each anode covered a 400 μm strip of the drift volume.

The read-out electronics consisted of a commercial hybrid pre-amplifier providing the first amplification stage, followed by a line driver and a shaping amplifier at the receiving end. Each shaping amplifier had two outputs: one bipolar for time measurement and a second gaussian for the charge measurement. The bipolar output wave form had the zero crossing corresponding to the time of arrival of the centre of gravity of the signal charge. This was input into a zero-crossing discriminator delivering the stop signal to a fast drift time recorder (DTR) with a 2μs time range started by the main trigger. At the test drift field of 724 V/cm, the full scale value of the drift time recorder allowed to cover 1.1cm distance in the drift direction.

For the charge measurement yielding the ionization of the particle, the gaussian output was recorded in a peak-sensing ADC. The recorded values of collected charge can be used for a precise determination of the second coordinate by the diffusing charge division method. The position in the direction perpendicular to the drift path is calculated by taking into account the centroid of the pulse heights recorded at different anodes, an upper limit of the resolution being determined by the width of the anode when the drift time si such that all the charge is collected in a single anode. In this test we were limited by the 400μm read-out pitch of the coupled anodes; 32 electronics channels were connected to 32 pair of anodes in the central part of the detector, thus covering a length of about 1.3 cm in the direction perpendicular to the drift.

Data analysis

In silicon drift detectors the electrons produced by the ionizing particle are focused at the centre of the detector slab by means of the depletion field and start drifting in the

direction of the anodes with a speed determined by the applied drift field. In the tests the charge produced by a traversing particle corresponded to about 250mV at the ADC.
While travelling towards the anodes the charge diffuses and is collected by several anodes. In order to reconstruct the total initial charge, the signal collected at contiguous anodes was added. Starting from the anode containing the highest signal above a "clustering threshold", typically 90 mV. The charges contained in all the neighbouring anodes were added to this initial charge. The addition of charges stopped when an anode containing less than a second threshold (30 mV) was encountered. The position of the cluster was found by computing the centre of gravity of the signal distribution seen at the anodes. The time (from the drift time recorders) measured at the anode containing the highest pulse height was taken as drift time.

The gain equalization of the electronic chains was done using the minimum ionizing particle signals with the requirement that the whole charge was seen at a single anode. For the specific purpose of analyzing the effect caused by doping fluctuations present in the 2 kΩcm silicon used [7,8,9], the time signals were equalized at the level of the first blade of the trigger counter. This was done by imposing that the mean value of the time distributions obtained from particles in the first scintillation detector blade corresponded to the same time.

The results

The raw time spectrum integrated over all the instrumented collecting anodes is shown in fig.2a. The structure introduced by the 100 μm wide blades of the trigger detector is clear. The particles reproduce the pattern of the blades detector in the solid state drift chamber. At the working field E_d=724 V/cm, the electrons drifts towards the collecting anodes with a velocity that we can estimate from this data by measuring the average time difference between two blade peaks. This is found to be 171 ns which with the known pitch of the blades (1000 μm) yields $v_d = 5.85\ 10^5$ cm/s. The resulting measured average drift mobility is thus:

$$\mu_d = v_d / E_d = 808\ cm^2/V\ s.$$

This shows that chamber was working at a high temperature as the mobility , which has a temperature dependence of $T^{-2.4}$, is lower than the expected at room temperature. The error on the calculated mobility is less than 10%, the mean width of the peaks of fig. 2a is taken as instrumental resolution.

Fig. 2b shows the time-of-arrival spectrum of particles depositing more than 150 mV in a single collecting pad. The peaks of fig.2b) are the result of a convolution of the

intrinsic chamber resolution, the width D of the corresponding blade, the beam divergence and the resolution of the time-measurement electronics.

Fig. 3 shows the measured width σ_τ of each time distribution from fig. 2b, corresponding to the blades of the trigger counter. Thus the variance of a peak σ_{tot} is given by;

$$\sigma^2_{tot} = (\sigma_\tau \times v_d)^2 = \sigma^2_{SiDD} + D^2/12 + \sigma^2_{el} + \sigma^2_{Beam}$$

where:

σ_τ	is the measured width of the time distribution;
v_d	is the the drift speed;
$D/\sqrt{12}$	is the contribution due to the width of a blade, (the effect of multiple scattering in the scintillation detector is negligible);
σ_{el}	is the resolution of the time measuring electronics (measured with a test pulse) $\sigma_{el} = 4$ ns; and
σ_{Beam}	is the contribution due to the beam divergence.

The beam is uniformly distributed on the blade counter, and has (approximately) a Gauss angular distribution with respect to the normal to the drift chamber plane, as determined by a Monte Carlo program that correctly reproduces the characteristics of the beam-line. Given the angular variance $\sigma_\theta = 0.13$ mrad and the distance between the blade scintillation detector and the drift detector, $l = 28$ cm , $\sigma_{Beam} = \sigma_\theta l = 36.4$ μm .

The intrinsic resolution of the detector in the drift direction can be estimated by finding the mean of the data points in fig. 3. This gives :

$$\sigma_{SiDD} = (40 \pm 10)\ \mu m,$$

Where the large error is due to the uncertainty with which the different contributions to be subtracted are known.

The relation time-distance relation is shown in fig.4 where the position of each triggering blade is plotted versus mean value of the drift-time distribution for the blade.

The results are in substantial agreement with the measures performed on the same detector with an IR laser. The linear response and resolution of this detector are known to be degraded due to the effects of doping fluctuations in the bulk material. A detailed treatment of doping fluctuations in this device is given in a previous paper [7].

The influence in the drift direction of the doping fluctuations is also evident from fig. 5 where the time of arrival of the electron clusters is plotted only for the pads having collected the largest pulse-height in the event. The line corresponding to the blade B1 has been equalized using the procedure described in the previous section. It can be seen that

this situation is not maintained for longer drift times. This affects the linear response at the level of 1–2% (fig. 4) and the position-resolution measurements for late-arriving clusters.

The front-end read out was not optimum as far as capacitance matching and energy resolution is concerned. The minimum ionizing peaks shown in fig.6, obtained with the clustering method mentioned above, suffers from this mismatch. Is evident though that the detector is still capable to separate a single particle from two overlapping particles. The threshold required to initiate a cluster was 90mV while the threshold determining the end of the cluster was 30mV.

In order show that no significant loss of charge occurred during the drift, the pulse heights recorded for early clusters ($t_{drift} \leq 0.8\mu s$, fig 6a) and for the late clusters ($t_{drift} > 1.2\ \mu s$, fig.6b) have been separately analyzed. The difference between the position of the peaks can be attributed to the clustering techniques used. Depending on the drift time the charge distribution is recorded on one or more anodes, for short drift time ($t_{drift} < 500$ ns) about 70% of the charge clusters where collected at one single coupled pair of anodes.

Conclusions

The silicon drift detector exposed to the beam had already been studied and characterized in detail. Beam tests intended to check the previous results in more realistic experimental conditions. These tests have shown all the strength of the drift detector as a position and ionization detector. The position resolution found in the drift direction was: $\sigma=(40 \pm 10)\ \mu m$. We could demonstrate that no significant charge loss occurred during the drift. The performance is limited by the doping fluctuations in the silicon. This results are encouraging us to proceed to a second production based on a slightly modified design and using higher-quality silicon material.

Acknowledgements

This work was supported in part by the U.S. Department of Energy, and the Italian INFN, MPI, and CNR.

We would like to thank K. Goulianos for his continuous support, L. Camilleri for his crucial help during the different phases of the test, C. Fabjan and K. Bussman for allowing us the use of the blade scintillation detector, and G. Stefanini for the use of the x y stage. We also thank W. Huta for careful mounting of the detector, and Marina Candusso and Fabrizio Massimo for the help during the collection of data.

References

[1] E. Gatti and P. Rehak, Nucl. Instr. and Meth. **A225** (1984) 608.

E. Gatti, P. Rehak and J.T. Walton, Nucl. Instr. and Meth. **226** (1984) 129.

[2] P. Rehak et al., Nucl. Instr. and Meth. **A248** (1986) 367.

[3] E. Gatti, P. Rehak and M. Sampietro, Nucl. Instr. and Meth. **A274** (1989) 469

[4] E. Gatti, P. Giacomelli, P. Holl, J. Kemmer, W. Kubischta, A. Longoni P. Rehak, M. Sampietro, L. Struder and A. Vacchi, Nucl. Instr. and Meth. **A273** (1988) 865.

[5] E. Gatti, A. Castoldi, S. Chinnici, A. Longoni, F. Palma, P. Rehak, M. Sampietro, and A. Vacchi, Nucl. Instr. and Meth. **A306** (1991) 187.

[6] E. Gatti, A. Castoldi, A. Longoni, M. Sampietro, P. Rehak and A. Vacchi ,Nucl. Instr. and Meth. **A295** (1990) 489

[7] A. Castoldi, S. Chinnici, E. Gatti, A. Longoni, M. Sampietro, P. Rehak, A. Vacchi, To appear in Journal of Applied Physics, April 92.

[8] W. v. Ammon and P. Dreier Wacker - Chemitronic GmbH, Proceeding of the 1988 International Symposium on Power Devices, ISPSD 88 Aug 22-23 1988 Tokyo pp. 134-140

[9] P. Dreier Wacker Chemitronic GmbH, FRG High Resistivity Silicon for Detector Applications Nucl. Inst. and Meth. **A228** (1990) 272.

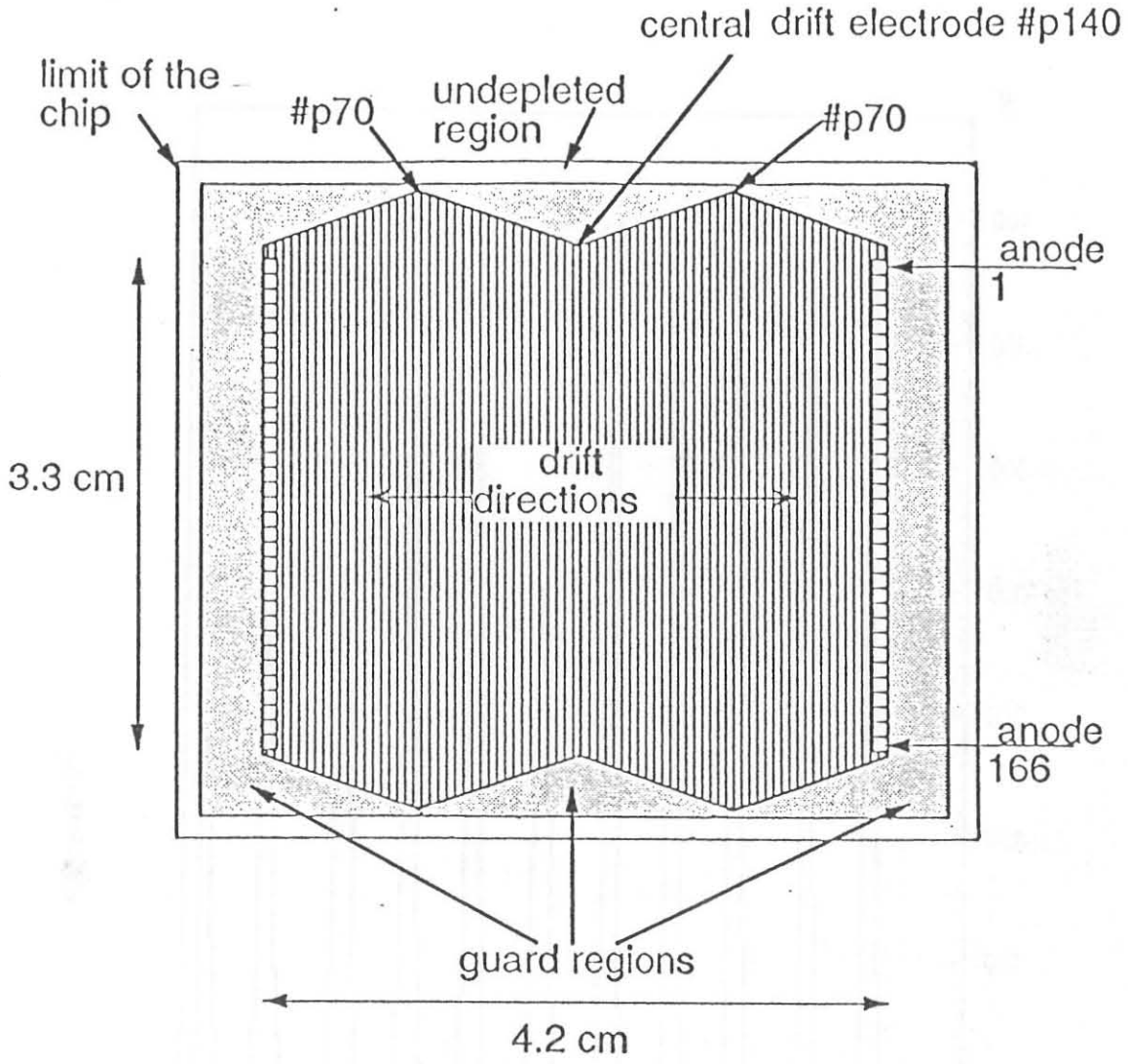

Fig. 1: Schematic drawing of the silicon drift detector.

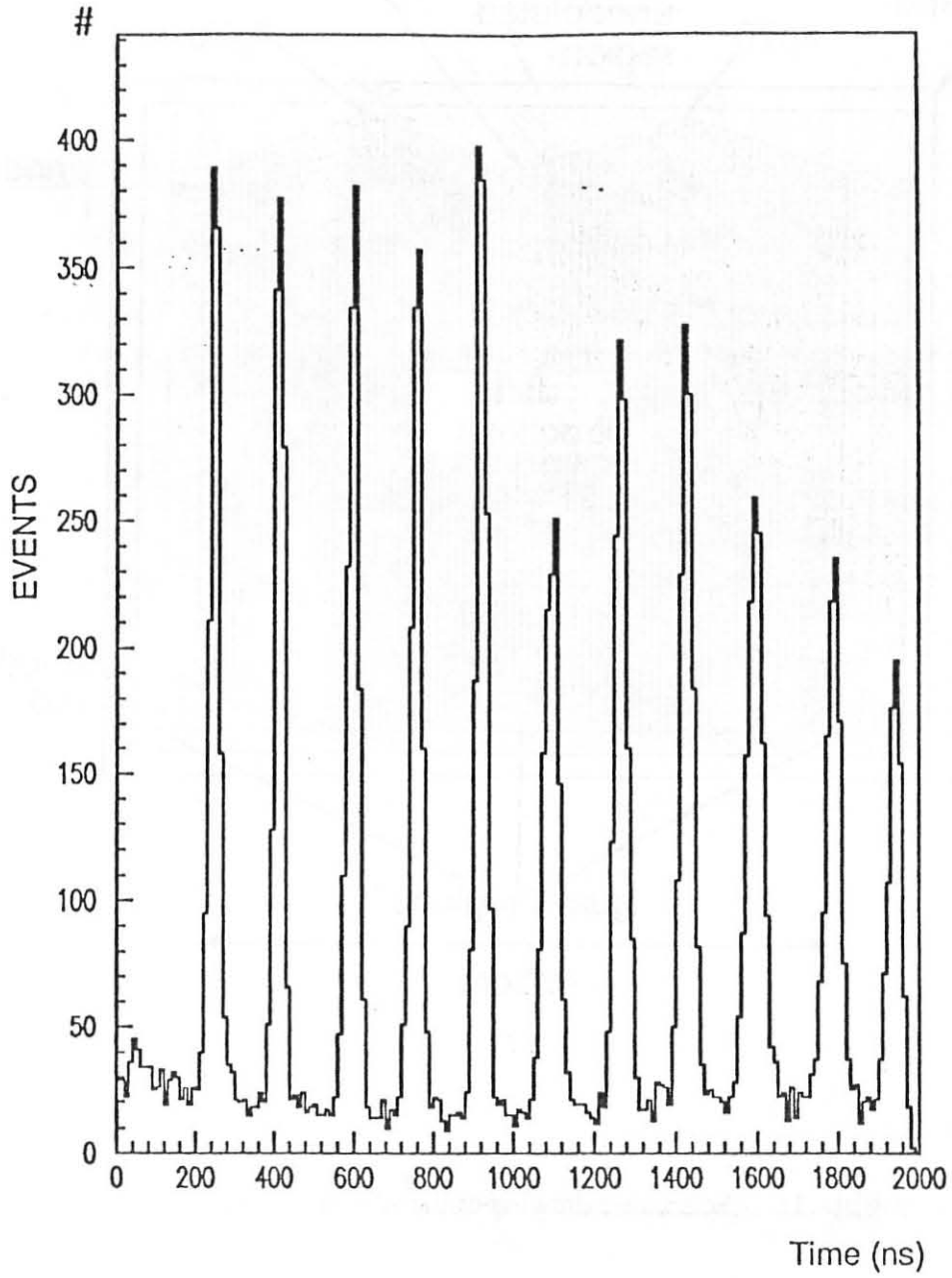

Fig. 2a: Raw data spectrum recorded at the Drift Time Recorders (DTR). This is a projection of the data recorded on all the instrumented anodes.

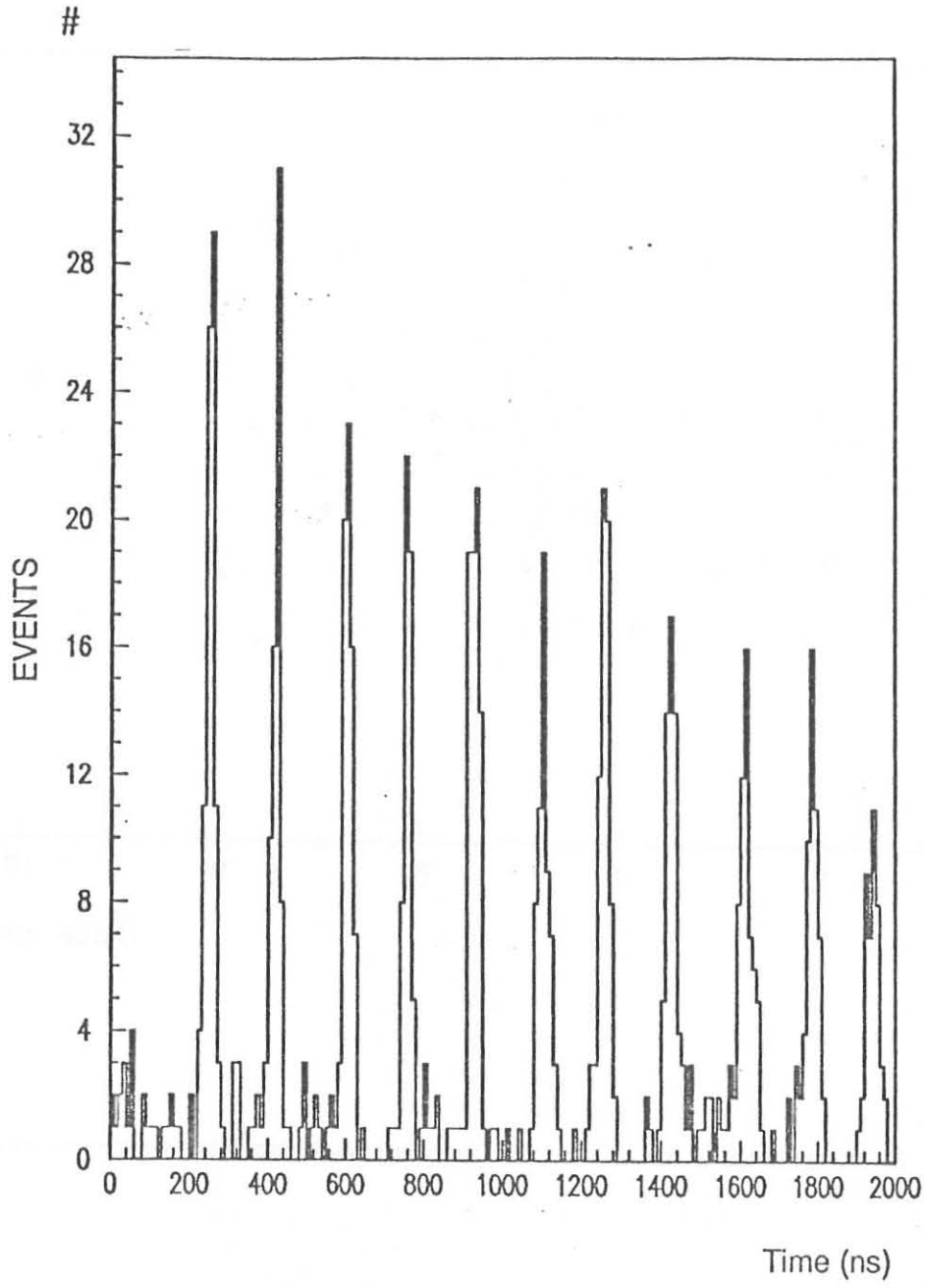

Fig. 2b: Time-of-arrival spectrum for the data recorded by one of the collecting anodes.

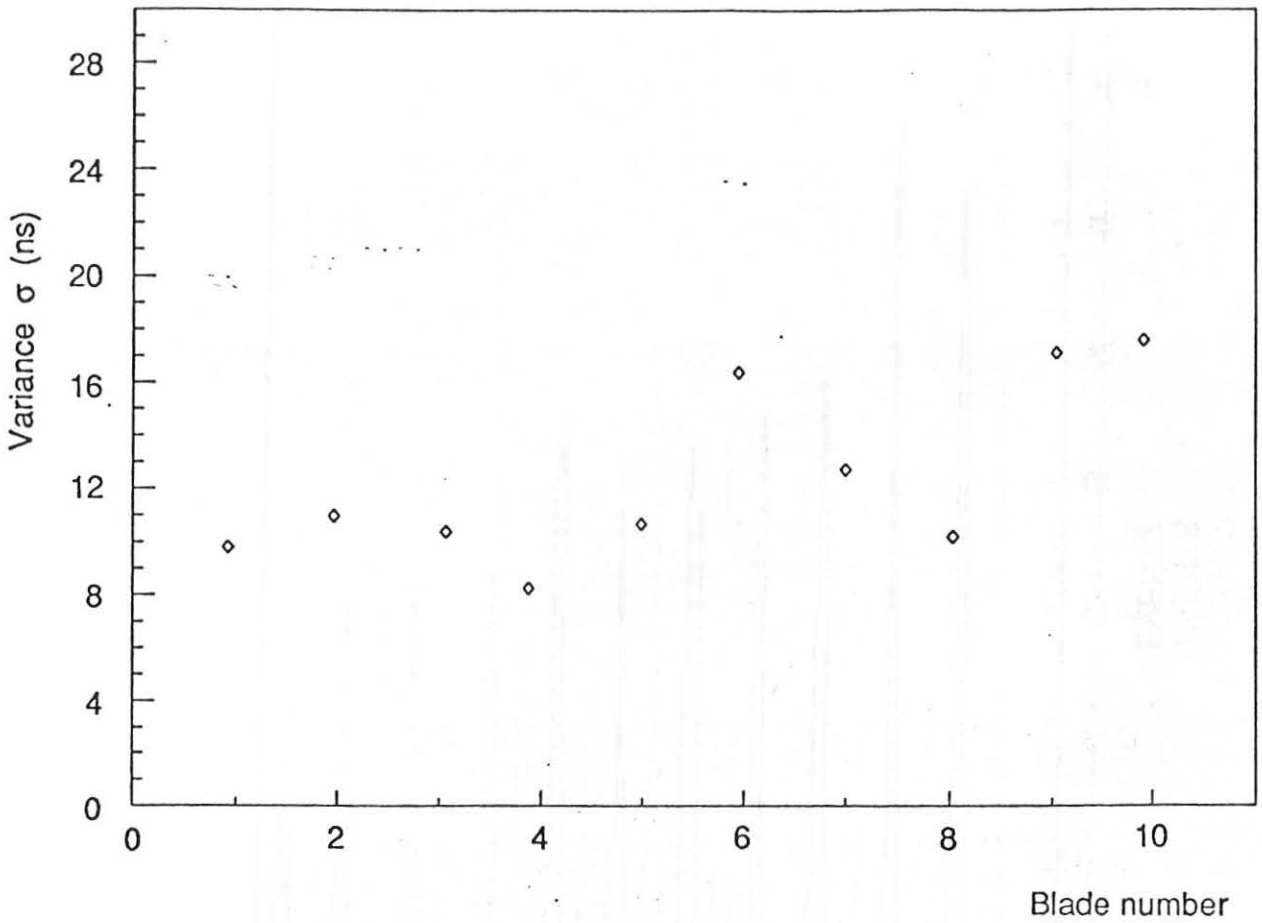

Fig. 3: SiDDσ_τ measured on all the time distributions induced by the trigger counter.

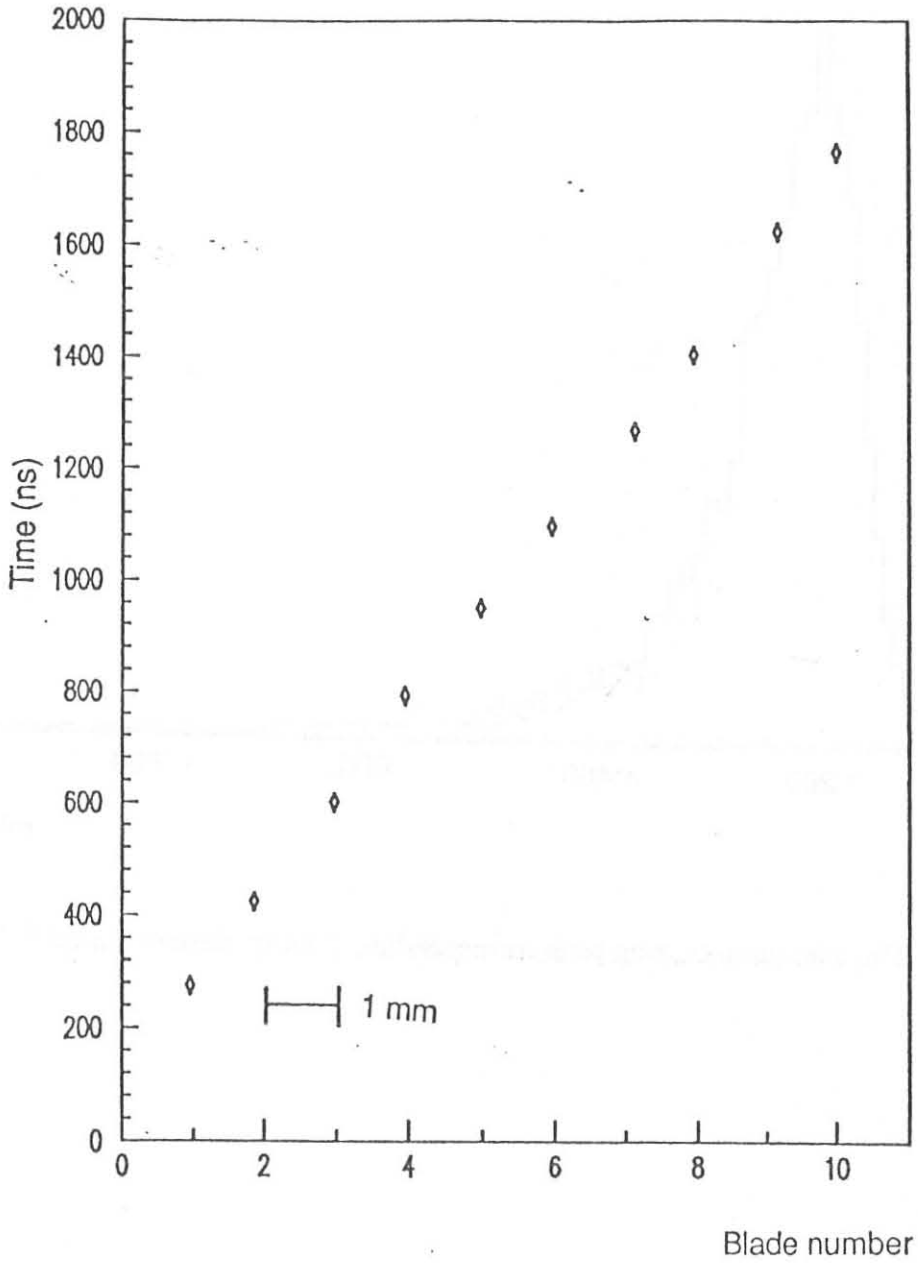

Fig. 4: Landau distribution of the minimum ionizing particles read out through peak sensitive ADC, 2a all clusters, 2b late arriving clusters.

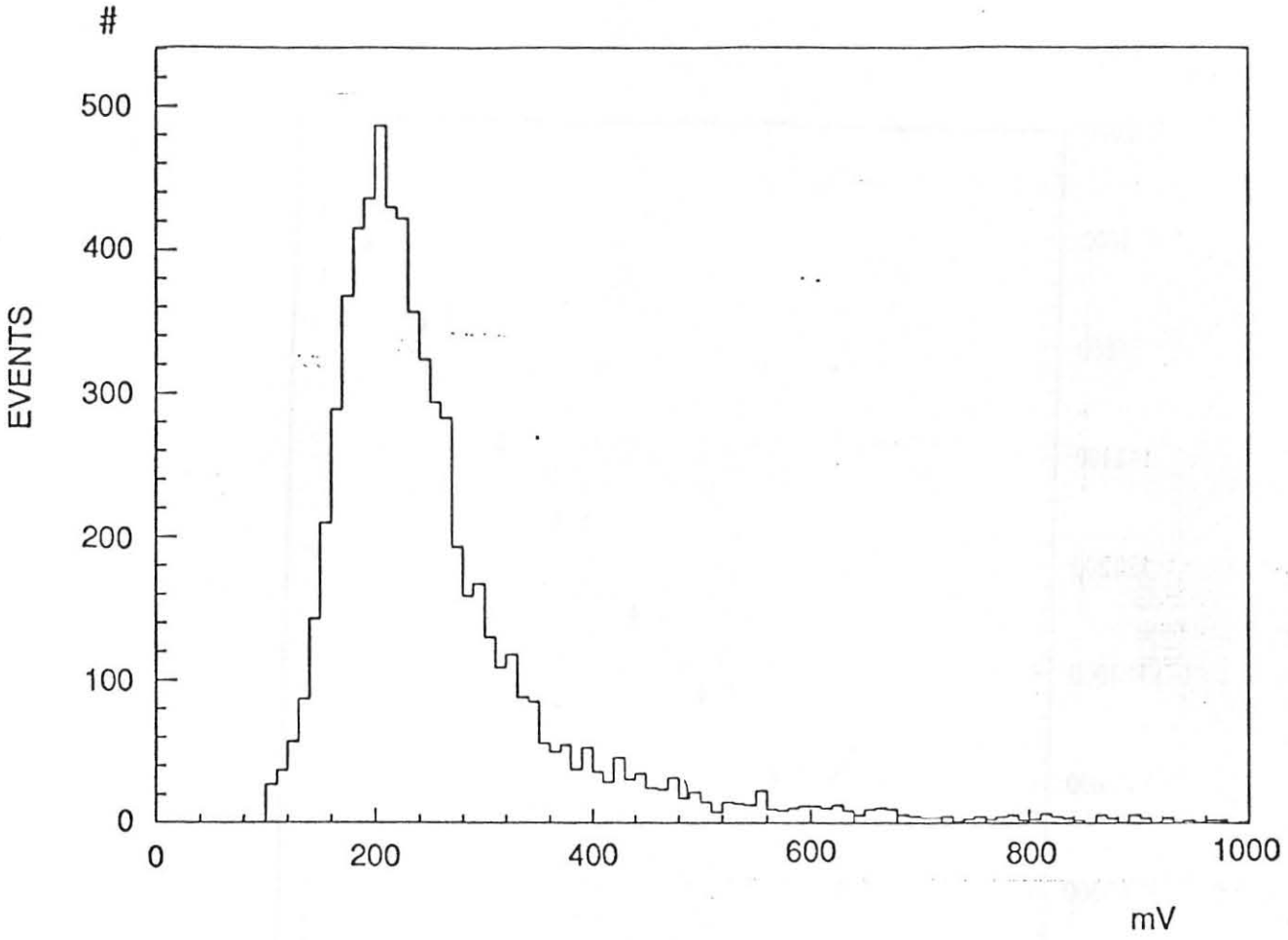

Fig. 6a: The minimum ionizing peak corresponding to early clusters ($t_{drift} \leq 0.8\mu s$).

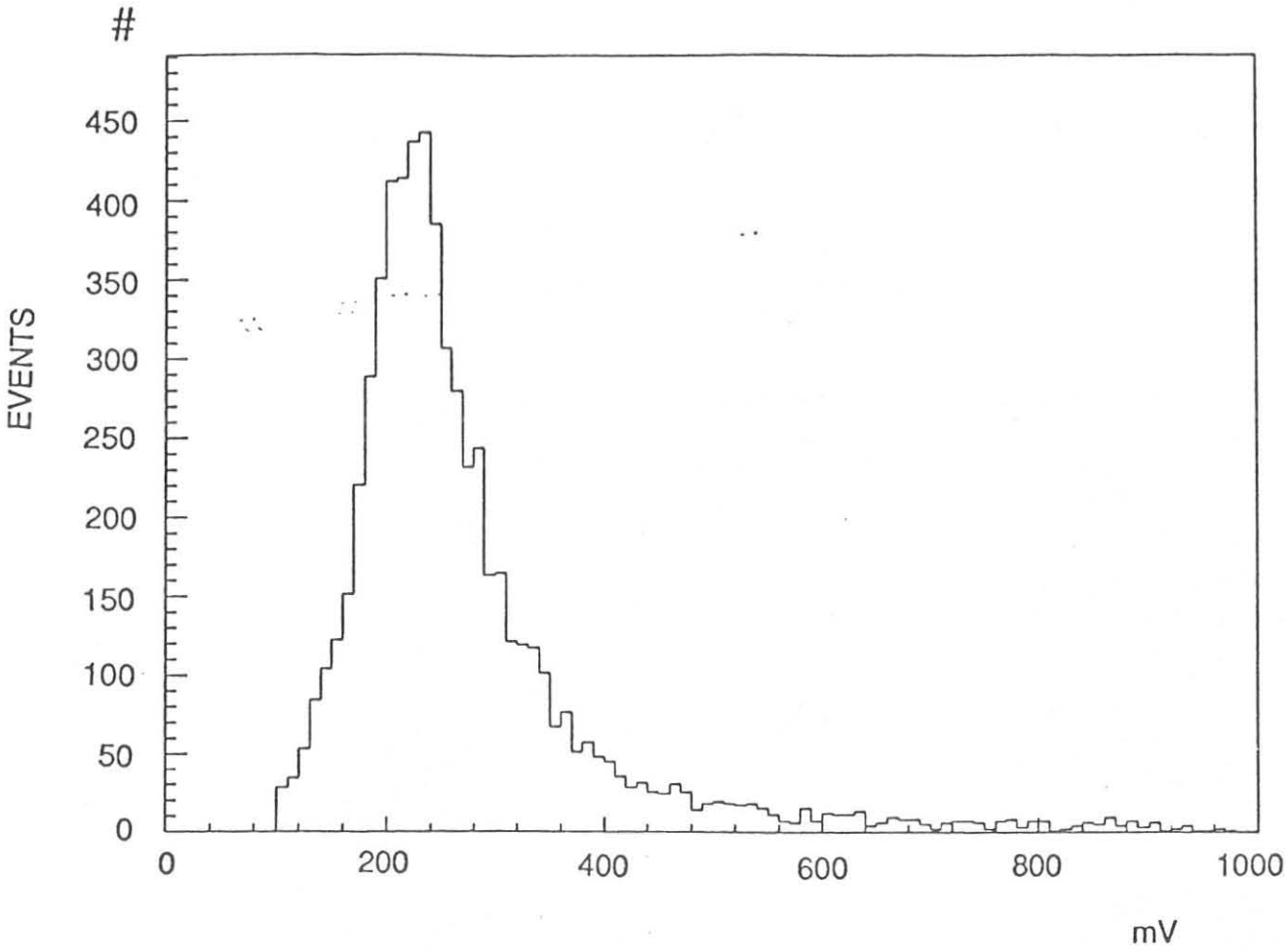

Fig. 6b: The pulse height obtained for the late clusters ($t_{drift} > 1.2\ \mu s$).